SMU
SINGAPORE MANAGEMENT UNIVERSITY

Lee Kong Chian School of Business

QF620 Stochastic Modelling in Finance

Project Report by Section G1 Team 1

Chan Ric, Kevin Montana Wongso, Nguyen Thanh Binh, Wong Jia Shing,
Yash Ashish Kumar Joshi, Zhang Yinliang

Part I (Analytical Option Formulae)

A vanilla option is a financial instrument that gives the holder the right, but not the obligation, to buy or sell an underlying asset at a predetermined price within a given timeframe. This option is a call/put option that has no special nor unusual features, meaning it is standardised if traded on an exchange, e.g., SGX. On the other hand, a digital cash/asset-or-nothing call (resp. put) is an option that has a binary outcome: it pays out either a fixed amount of one unit of cash/asset, if the underlying stock becomes above (resp. below) a predetermined threshold or strike price, or pays out nothing.

Let $Z \sim N(0,1)$ be the standard normal random variable, whose probability density function (PDF) is given by $\phi(z) = \frac{1}{\sqrt{2\pi}} e^{-\frac{z^2}{2}}$. Define its cumulative distribution function (CDF) by $\Phi(z) = \int_{-\infty}^{z} \phi(z')\, dz'$.

In the displaced-diffusion model, the factor $\beta \in [0,1]$ plays a significant role in modifying the underlying asset's price S_0's dynamics, meaning β controls the degree to which S_0 influences the asset's volatility:

- $\beta = 1$: The model reduces to the standard Black-Scholes model, where the volatility term is simply σS_0, meaning the volatility is proportional to the asset's/stock's price.
- $\beta = 0$: The model's dynamics are dominated by the constant F_0, making the volatility independent of the asset's/stock's price. This implies the volatility term becomes σF_0.
- $0 < \beta < 1$: The model incorporates a blend of both the asset's/stock's price S_0 and the constant F_0. This allows the model to capture scenarios where the volatility is not entirely proportional to the asset's/stock's price but is also influenced by some baseline, represented by F_0.

In general, a higher β implies the volatility is more strongly tied to the asset's/stock's price, while a lower β suggests the volatility is more dependent on the constant F_0. This flexibility makes the displaced-diffusion model useful in modelling situations where the asset's/stock's price volatility does not behave purely as a linear function of its current price.

We first define the following variables:

t: the time in years, where $t \geq 0$; assuming WLOG that $t = 0$ represents the current year,

r: the annual continuously compounded risk-free interest rate,

S_0: the initial asset/stock price,

μ: the annual drift rate of S_0,

σ: the standard deviation of the stock's returns, i.e., the square root of the quadratic variation of the stock's log price process (measure of stock's volatility),

T: the expiry date of the option, i.e., $0 \leq t \leq T$.

K: the at-the-money (ATM) strike price of the option,

F_0: the initial discounted futures price ($F_0 = S_0 e^{rT}$).

Using these definitions, we derive (see `part1.ipynb`) and define the following equations for the prices of the European options at expiry date T under the respective option pricing models:

Model	Option type		
	Vanilla call/put	Digital cash-or-nothing call/put	Digital asset-or-nothing call/put
Black-Scholes $d_1 = \frac{\log\frac{S_0}{K} + \left(r + \frac{\sigma^2}{2}\right)T}{\sigma\sqrt{T}}$ $d_2 = d_1 - \sigma\sqrt{T}$	Call: $C_{BS,v} = S_0\Phi(d_1) - Ke^{-rT}\Phi(d_2)$ Put: $P_{BS,v} = Ke^{-rT}\Phi(-d_2) - S_0\Phi(-d_1)$	Call: $C_{BS,c} = e^{-rT}\Phi(d_2)$ Put: $P_{BS,c} = e^{-rT}\Phi(-d_2)$	Call: $C_{BS,a} = S_0\Phi(d_1)$ Put: $P_{BS,a} = S_0\Phi(-d_1)$
Bachelier $d = \frac{S_0 - K}{\sigma\sqrt{T}}$	$C_{Ba,v} = e^{-rT}\left[(S_0 - K)\Phi(d) + \sigma\sqrt{T}\phi(d)\right]$ $P_{Ba,v} = e^{-rT}\left[(K - S_0)\Phi(-d) + \sigma\sqrt{T}\phi(-d)\right]$	$C_{Ba,c} = e^{-rT}\Phi(d)$ $P_{Ba,c} = e^{-rT}\Phi(-d)$	$C_{Ba,a} = S_0\Phi(d) + \sigma\sqrt{T}\phi(d)$ $P_{Ba,a} = S_0\Phi(-d) + \sigma\sqrt{T}\phi(-d)$
Black $d_1 = \frac{\log\frac{F_0}{K} + \frac{\sigma^2}{2}T}{\sigma\sqrt{T}}$ $d_2 = d_1 - \sigma\sqrt{T}$	$C_{B,v} = e^{-rT}\left[F_0\Phi(d_1) - K\Phi(d_2)\right]$ $P_{B,v} = e^{-rT}\left[K\Phi(-d_2) - F_0\Phi(-d_1)\right]$	$C_{B,c} = e^{-rT}\Phi(d_2)$ $P_{B,c} = e^{-rT}\Phi(-d_2)$	$C_{B,a} = F_0e^{-rT}\Phi(d_1)$ $P_{B,a} = F_0e^{-rT}\Phi(-d_1)$
Displaced-diffusion $d_1 = \frac{\log\left(\frac{F_0}{F_0 + \beta(K - F_0)}\right) + \frac{(\sigma\beta)^2}{2}T}{\sigma\beta\sqrt{T}}$ $d_2 = d_1 - \sigma\beta\sqrt{T}$	$C_{D,v} = C_{B,v}\left(\frac{F_0}{\beta}, K + \frac{1-\beta}{\beta}F_0, r, \beta\sigma, T\right)$ $= e^{-rT}\left[\frac{F_0}{\beta}\Phi(d_1) - \left(K + \frac{1-\beta}{\beta}F_0\right)\Phi(d_2)\right]$ $P_{D,v} = P_{B,v}\left(\frac{F_0}{\beta}, K + \frac{1-\beta}{\beta}F_0, r, \beta\sigma, T\right)$ $= e^{-rT}\left[\left(K + \frac{1-\beta}{\beta}F_0\right)\Phi(-d_2) - \frac{F_0}{\beta}\Phi(-d_1))\right]$	$C_{D,c} = e^{-rT}\Phi(d_2)$ $P_{D,c} = e^{-rT}\Phi(-d_2)$	$C_{D,a} = \frac{F_0}{\beta}\Phi(d_1)$ $P_{D,a} = \frac{F_0}{\beta}\Phi(-d_1)$

These models are used to evaluate different types of options under varying assumptions about the underlying asset's volatility, time to maturity, and the relationship between volatility and the asset price. Our key focus here is on how the underlying assumptions affect the option prices.

Substituting $K = 85$, $r = 5\% = 0.05$, $\sigma = 0.40$, $T = 0.2$ and $\beta = 0.3$ into the equations defined above, we compute each of the option prices using Python and obtain the following results:

S_0	$C_{BS,v}$	$P_{BS,v}$	$C_{BS,c}$	$P_{BS,c}$	$C_{BS,a}$	$P_{BS,a}$	$C_{Ba,v}$	$P_{Ba,v}$	$C_{Ba,c}$	$P_{Ba,c}$	$C_{Ba,a}$	$P_{Ba,a}$
80	4.005	8.159	0.351	0.639	33.861	46.139	0	4.950	0	0.990	0	80
90	9.560	3.714	0.606	0.384	61.109	28.891	4.950	0	0.990	0	90	0

S_0	$C_{B,v}$	$P_{B,v}$	$C_{B,c}$	$P_{B,c}$	$C_{B,a}$	$P_{B,a}$	$C_{D,v}$	$P_{D,v}$	$C_{D,c}$	$P_{D,c}$	$C_{D,a}$	$P_{D,a}$
80	4.005	8.159	0.351	0.639	33.861	46.139	3.913	8.067	0.373	0.617	105.857	160.81
90	9.560	3.714	0.606	0.384	61.109	28.891	9.705	3.859	0.627	0.363	195.909	104.091

The table demonstrates how different models handle the pricing of both vanilla and digital options, illustrating how volatility and the relationship between the asset price and volatility can affect option values. Under the Black-Scholes model applied to the vanilla options, we see that for a lower initial stock price ($S_0 = 80$), the call option is cheaper, while the put option is more expensive. This is expected as the stock price is below the strike price ($K = 85$). Conversely, when the stock price rises above the strike price ($S_0 = 90$), the call option becomes more valuable while the put option becomes cheaper. On the other hand, digital options offer binary outcomes − either a fixed cash or asset payout if the option is in the money (the asset price crosses the strike price), or nothing otherwise. Specifically, the prices for cash-or-nothing options and asset-or-nothing options reflect the probabilities of these binary outcomes. These prices under different models vary depending on how each model captures volatility and the underlying asset's price dynamics. For example, under the Bachelier model, the prices for asset-or-nothing options are significant due to the model's assumption of a linear Brownian motion for asset prices. Finally, the prices calculated under the displaced-diffusion model show how introducing displacement affects the valuation of options. For instance, the prices for digital options under this model are different from those in the Black-Scholes model, highlighting the impact of β on option pricing. This property allows the displaced-diffusion model to capture situations where volatility does not strictly follow the asset price, offering a more flexible framework for option pricing. Overall, these insights help traders and risk managers choose the most appropriate model for their needs, depending on the asset's characteristics and the type of options being priced.

Part II (Model Calibration)

On `1-Dec-2020`, the S&P 500 (SPX) index value was 3662.45, while the SPDR S&P 500 Exchange Traded Fund (SPY) stock price was 366.02. The call and put option prices (bid & offer) over 3 maturities are provided in the spreadsheets `SPX_options.csv` and `SPY_options.csv`. The discount rate on this day is in the file `zero_rates_20201201.csv`. To obtain the market-implied volatility smile, we first compute it under the Black-Scholes model by extracting the implied volatilities from the option prices observed in the market. This process involves finding the volatility parameter σ in the Black-Scholes formulae that equate the theoretical option price to the market price for each strike price and maturity. The Black-Scholes formulae themselves assume constant volatility, but the variation in implied volatility across different strike prices, known as the volatility smile, reflects deviations from this assumption in real markets.

We start by gathering the relevant data for the S&P 500 index and its associated SPDR ETF options. This includes the option prices (both bid and offer) for several strike prices and maturities, as well as the risk-free discount rates for the respective maturities, provided in the `zero_rates_20201201.csv` file. Using the given SPX and SPY option price data from the provided spreadsheets (`SPX_options.csv`, `SPY_options.csv`), we proceed with the calculation of implied volatility. To do this, we reverse-engineer the Black-Scholes formulae. By solving numerically for σ using Brent's method (coded as `brentq`) as computed in our Jupyter Notebook, we obtain the implied volatility for each option. Once this is done across all available options, we plot these against the strike prices for each maturity as shown below.

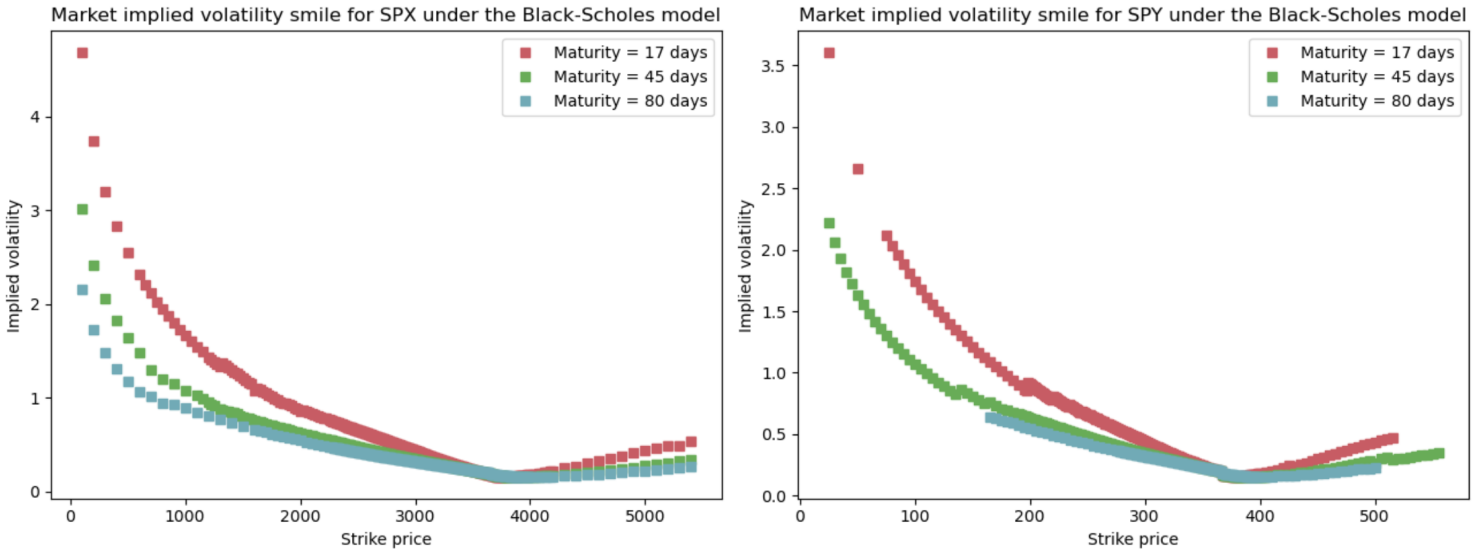

Here, we observe distinct market-implied volatility smiles for different maturities. In the Black-Scholes framework, implied volatility should theoretically remain constant across strike prices for a given maturity, assuming that the model's assumption of constant volatility holds. However, the graphs reveal a clear deviation from this assumption, as we see a pronounced smile or skew, indicating that implied volatility varies significantly with strike prices. From the SPX chart, we observe that for all maturities (17, 45 and 80 days), the implied volatility is significantly higher for lower strike prices and gradually decreases as the strike price increases, reaching a minimum around the at-the-money (ATM) strikes. Beyond the ATM region, the volatility starts increasing again slightly for higher strike prices, forming a typical volatility smile pattern. This pattern is most pronounced for shorter maturities (e.g., 17 days) and becomes flatter as the maturity increases. The SPY chart shows a similar pattern, though the scale of implied volatilities is lower compared to SPX. The

implied volatility remains high for out-of-the-money (OTM) put options, reflecting a similar smile shape. Additionally, the skew is steeper for shorter maturities, especially at lower strike prices. This suggests that the market is pricing in more risk or uncertainty for SPY options with shorter maturities and for strikes that are further from the current spot price.

The shape of the volatility smile in both cases allows us to infer important market expectations. Higher implied volatility for OTM options, particularly for puts, indicates that the market anticipates significant price movements or possible downside risk in the underlying asset. In contrast, the flatter portion of the smile near ATM strikes suggests that the market expects relatively stable volatility near current levels. The skewed nature of the volatility smile suggests an asymmetric view of risk, where the market might be hedging against large downward movements in price, especially for shorter-dated options. These observations reflect the market's expectations of future volatility and risk. The pronounced skew in shorter maturities points to heightened uncertainty or anticipated market movements in the near term, particularly at lower strike prices. These observations provide critical insights that inform more sophisticated option pricing models, such as the displaced-diffusion and SABR models, which address the limitations of the Black-Scholes (or simply lognormal) assumption of constant volatility.

Next, to match the option prices, we calibrate both models: displaced-diffusion and SABR ($\beta = 0.7$). The implied volatility of the SABR model is given by:

$$\begin{aligned}
&\sigma_{\text{SABR}}(F_0, K, \alpha, \beta, \rho, \nu) \\
&= \frac{\alpha}{(F_0K)^{(1-\beta)/2}\left\{1 + \frac{(1-\beta)^2}{24}\log^2\left(\frac{F_0}{K}\right) + \frac{(1-\beta)^4}{1920}\log^4\left(\frac{F_0}{K}\right) + \cdots\right\}} \\
&\quad \times \frac{z}{x(z)} \times \left\{1 + \left[\frac{(1-\beta)^2}{24}\frac{\alpha^2}{(F_0K)^{1-\beta}} + \frac{1}{4}\frac{\rho\beta\nu\alpha}{(F_0K)^{(1-\beta)/2}} + \frac{2-3\rho^2}{24}\nu^2\right]T + \cdots\right\},
\end{aligned}$$

where $z = \frac{\nu}{\alpha}(F_0K)^{(1-\beta)/2}\log\left(\frac{F_0}{K}\right)$ and $x(z) = \log\left[\frac{\sqrt{1-2\rho z+z^2}+z-\rho}{1-\rho}\right]$. Define the errors:

$$\begin{cases}
\sigma_{\text{Mkt}}(K_i) - \sigma_{\text{D}}(F_0, K_i, r, \sigma_i, T, \beta, \text{payoff}) & = \epsilon_i^{\text{D}}, \\
\sigma_{\text{Mkt}}(K_i) - \text{SABR}(F_0, K_i, T, \alpha, \beta, \rho, \nu) & = \epsilon_i^{\text{SABR}},
\end{cases}$$

for $i = 1, \ldots, n$, where n is the total number of data points of K. Then, we use the `least_squares` algorithm in the `scipy` module to calibrate the displaced-diffusion and SABR model parameters by minimising the sum of squared error terms, i.e., via $\min\limits_{\sigma,\,\beta} \sum_{i=1}^{n}(\epsilon_i^D)^2$ and $\min\limits_{\alpha,\,\rho,\,\nu} \sum_{i=1}^{n}(\epsilon_i^{\text{SABR}})^2$ respectively. In the process, we report the following model parameters as shown below:

1. displaced-diffusion: σ, β,
2. SABR: α, ρ, ν.

	SPX, 17 days	SPX, 45 days	SPX, 80 days	SPY, 17 days	SPY, 45 days	SPY, 80 days
σ	0.212	1.003	2.025	0.030	0.149	1.846
β	0.958	0.917	0.878	0.925	0.823	0.286

Table 1: Calibrated values under the displaced-diffusion model

	SPX, 17 days	SPX, 45 days	SPX, 80 days	SPY, 17 days	SPY, 45 days	SPY, 80 days
α	1.212	1.817	2.140	0.665	0.908	1.121
ρ	-0.301	-0.404	-0.575	-0.412	-0.489	-0.633
ν	5.460	2.790	1.842	5.250	2.729	1.742

Table 2: Calibrated values under the SABR model

Finally, we plot the fitted implied volatility smiles against the market data below:

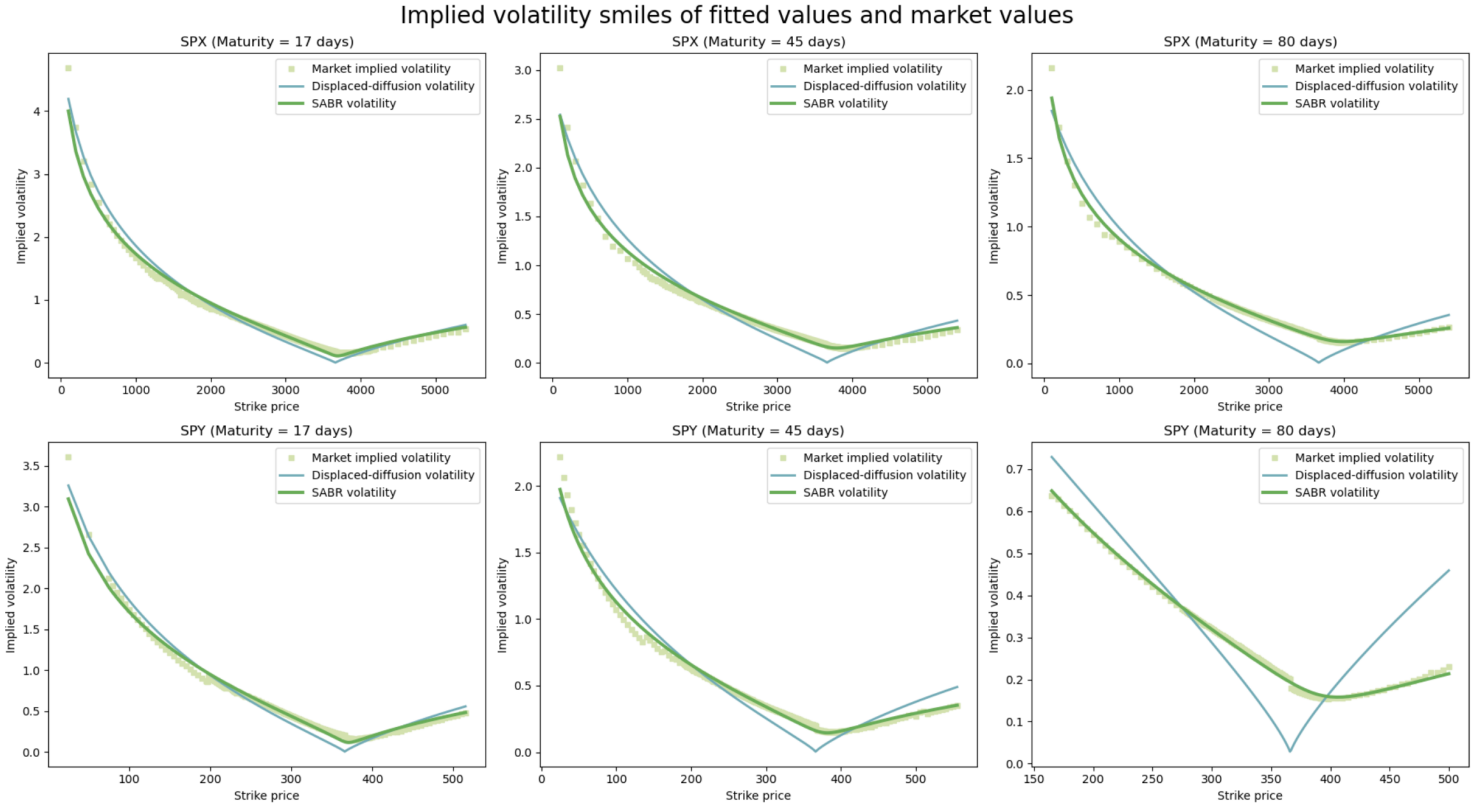

We can see how each of the two models employs specific parameters to adjust the shape and characteristics of the implied volatility smile, which reflects how market volatility varies across different strike prices. Firstly, the displaced-diffusion model introduces a parameter, β, which controls the level of displacement from the lognormal model. The changes in β directly impact the curvature and skewness of the implied volatility smile. A lower β (closer to 0) makes the model behave more like a lognormal model. As a result, the implied volatility smile exhibits more pronounced curvature, especially for OTM and in-the-money (ITM) options. Volatility is higher for OTM and ITM options compared to ATM options, making the smile more pronounced. This steeper volatility smile indicates that the market perceives higher risk for extreme strike prices. On the other hand, as β approaches 1, the model behaves more like the standard Black-Scholes model. This results in a flatter volatility smile, with reduced skewness and curvature. Volatility becomes more uniform across different strike prices, indicating that the market perceives less variation in volatility across strikes. From the graphs above, we observe that higher β values reduce the steepness of the smile, aligning with the flatter shapes depicted by the Black-Scholes model for ATM options. For β closer to 0, the volatility is significantly higher for OTM and ITM options.

For the case of the SABR model, α is a key parameter that primarily affects the level of volatility, while ρ and ν influence the skewness and steepness of the volatility smile. In particular, α represents the initial level of volatility in the SABR model. Adjusting α changes the overall height of the volatility smile. For instance, a higher α reflects a general increase in implied volatility across strike prices. This is common in markets with high volatility, characterised by steeper implied volatility curves. In contrast, a lower α reduces the overall level of implied volatility, making the volatility smile flatter and closer to the baseline Black-Scholes curve. This could represent a market with lower volatility or where the volatility of the underlying asset is perceived as stable. Besides, ρ (measure of correlation between the asset price and volatility) controls the skewness of the volatility smile. Negative ρ values lead to a right-skewed volatility smile (downward slope), while positive ρ results in a left-skewed smile (upward slope). Moreover, ν (volatility of volatility) influences the overall curvature and steepness of the volatility smile. In particular, a higher ν increases the variability in implied volatility, making the smile more pronounced, while lower ν flattens the smile. From the graphs above, we see that α directly influences the height of the SABR-implied volatility smile, with higher values of α leading to a uniformly higher implied volatility curve. The combined interaction between ρ and ν shapes the smile's skewness and steepness, making the SABR model more flexible than Black-Scholes in capturing market behaviors across different strike prices.

In general, the model parameters calibrated allow both models to capture various features of the implied volatility smile alongside the market conditions that affect it, making these parameters useful tools in the calibration of option pricing models to market data.

Part III (Static Replication)

Suppose on `1-Dec-2020`, we wish to evaluate an exotic European derivative expiring on `15-Jan-2021` with payoff function given by $h(S_T) = S_T^{1/3} + 1.5 \times \log(S_T) + 10.0$ and "model-free" integrated variance given by $\sigma_{\text{MF}}^2 T = \mathbb{E}\left[\int_0^T \sigma_t^2 \, dt\right]$. To do this, we compute a suitable value of $\sigma = \sigma_{\text{MF}}$ corresponding to SPX and SPY under each of the Black-Scholes, Bachelier and SABR models (as calibrated in Part 2). We first take the first-order and second-order derivatives of h to obtain:

$$h'(S_T) = \frac{1}{3} S_T^{-\frac{2}{3}} + \frac{3}{2} S_T^{-1}, \quad h''(S_T) = -\frac{2}{9} S_T^{-\frac{5}{3}} - \frac{3}{2} S_T^{-2}.$$

Then, by substituting relevant results from Parts 1-2 to the formula for the derivative contract:

$$V_0 = e^{-rT} h(F) + \underbrace{\int_0^F h''(K) P(K) \, dK}_{\text{put integral}} + \underbrace{\int_F^\infty h''(K) C(K) \, dK}_{\text{call integral}},$$

as well as the "model-free" integrated variance equation under static replication:

$$E = \mathbb{E}\left[\int_0^T \sigma_t^2 \, dt\right] = 2e^{rT} \left(\int_0^F \frac{P(K)}{K^2} \, dK + \int_F^\infty \frac{C(K)}{K^2} \, dK \right),$$

we obtain, by numerical integration using the Gaussian quadrature rule (coded as `quad`), the following results:

	SPX (BS)	SPY (BS)	SPX (Bachelier)	SPY (Bachelier)	SPX (SABR)	SPY (SABR)
V_0	37.670	25.963	37.703	25.978	37.700	25.993
E	0.0184	0.0248	0.0052	0.0151	0.0063	0.0060
σ^2_{MF}	0.149	0.201	0.042	0.122	0.051	0.049
σ	0.386	0.448	0.205	0.350	0.227	0.221

We see that the SABR model yields slightly higher prices for SPX and similar results for SPY compared to the other models. The slight differences in V_0 between the models indicate that while the Black-Scholes, Bachelier and SABR models may share certain similarities in pricing the exotic derivative, the SABR model captures a bit more market dynamics (such as volatility skew) than the simpler Black-Scholes and Bachelier models. Moreover, based on the expected integrated variance data obtained, the SABR model measures and predicts less stochastic volatility over the life of the derivative compared to the constant volatility assumed in the Black-Scholes and Bachelier models. Furthermore, the variation in model-free integrated variance highlights how the Black-Scholes model, which assumes constant volatility, overestimates total variance compared to the stochastic volatility captured by the SABR model. Finally, the Black-Scholes model consistently estimates higher σ than both the Bachelier and SABR models. This suggests that Black-Scholes may overestimate the potential risk, while the SABR model, which captures the volatility skew, provides a more nuanced and realistic volatility estimate for both SPX and SPY. Overall, these findings suggest that the SABR model is more adept at capturing market nuances such as volatility smiles and skews, providing a more realistic estimate of derivative pricing and volatility for both SPX and SPY options.

Part IV (Dynamic Hedging)

Black-Scholes introduced the notion of dynamic delta hedging − by executing delta hedges instantaneously, we ensure that our portfolio is delta neutral, and consequently hedged the exposure of our call position using the underlying stock and the risk-free bond. Suppose $S_0 = 100$, $\sigma = 0.2$, $r = 5\%$, $T = \frac{1}{12}$ year, i.e. 1 month, and $K = 100$. Suppose we sell a stock's ATM call option under the Black-Scholes model, and we hedge it N times during its life. The dynamic hedging strategy for an option is $C_t = \phi_t S_t - \psi_t B_t$, where $\phi_t = \frac{\partial C}{\partial S} = \Phi\left(\frac{\log\left(\frac{S_t}{K}\right)+\left(r+\frac{1}{2}\sigma^2\right)(T-t)}{\sigma\sqrt{T-t}}\right)$, and $\psi_t B_t = -Ke^{-r(T-t)}\Phi\left(\frac{\log\left(\frac{S_t}{K}\right)+\left(r-\frac{1}{2}\sigma^2\right)(T-t)}{\sigma\sqrt{T-t}}\right)$. Assuming there are 21 trading days over the month, we consider five different numbers of steps (expressed in days): 21, 42, 105, 210, 420; to simulate the stock price. By performing Monte-Carlo simulations involving 10^6 steps per simulation using `simulate_Brownian_Motion(paths, steps, T)` on our Jupyter Notebook, we obtain these results:

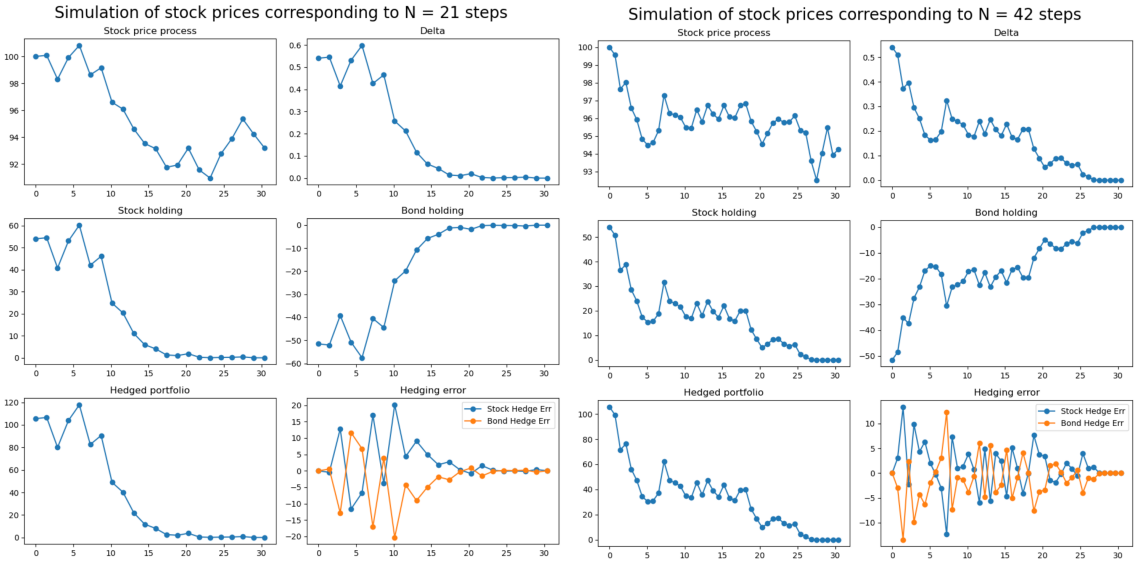
Simulation of stock prices corresponding to N = 21 steps
Stock price process
Delta
Stock holding
Bond holding
Hedged portfolio
Hedging error
Stock Hedge Err
Bond Hedge Err
Simulation of stock prices corresponding to N = 42 steps
Stock price process
Delta
Stock holding
Bond holding
Hedged portfolio
Hedging error
Stock Hedge Err
Bond Hedge Err

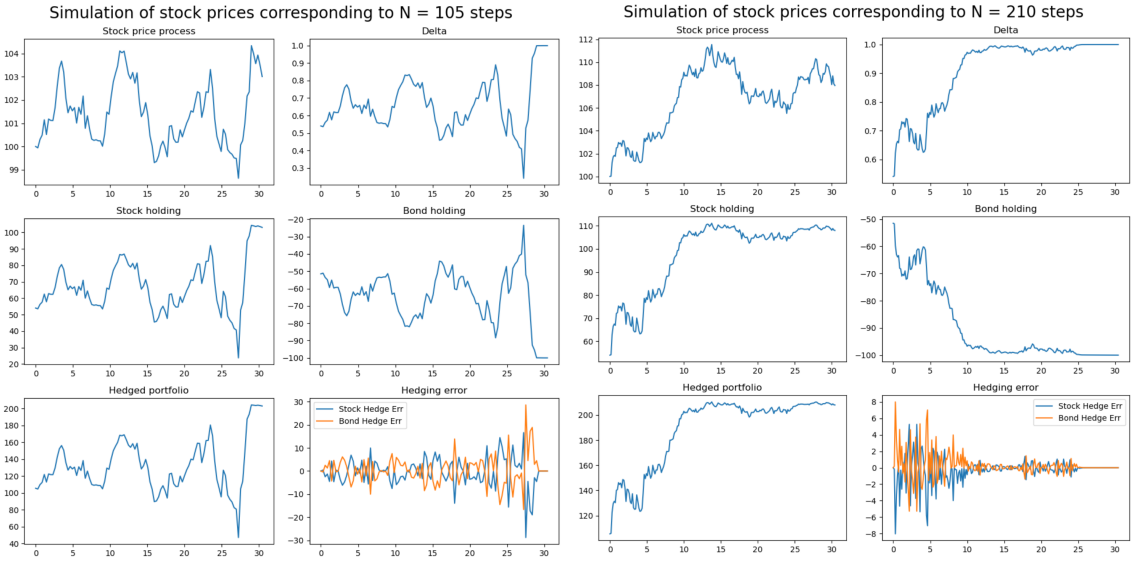
Simulation of stock prices corresponding to N = 105 steps
Stock price process
Delta
Stock holding
Bond holding
Hedged portfolio
Hedging error
Stock Hedge Err
Bond Hedge Err
Simulation of stock prices corresponding to N = 210 steps
Stock price process
Delta
Stock holding
Bond holding
Hedged portfolio
Hedging error
Stock Hedge Err
Bond Hedge Err

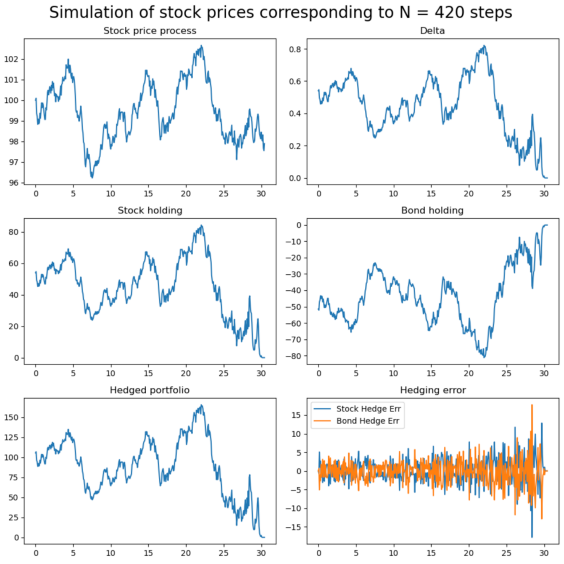
Simulation of stock prices corresponding to N = 420 steps
Stock price process
Delta
Stock holding
Bond holding
Hedged portfolio
Hedging error
Stock Hedge Err
Bond Hedge Err

The dynamic delta hedging strategy is designed to manage the risk associated with holding a call option by continuously adjusting the portfolio's exposure to the underlying stock and bond. The results above demonstrate the performance of this strategy across various numbers of hedging steps over the life of the option. The simulations illustrate the evolution of key variables such as the stock price, delta, stock and bond holdings, the value of the hedged portfolio, and the hedging error.

Across all simulations, the stock price follows a stochastic process, modeled using Brownian motion, with some variability but generally trending close to its starting price of $S_0 = 100$. As the number of steps N increases, the stock price appears to fluctuate more smoothly, which is consistent with a finer resolution of time increments in the simulation. For example, the stock price path for $N = 420$ is smoother compared to $N = 21$, where fluctuations are more pronounced due to larger step sizes. Moreover, the delta (represents the sensitivity of the option price to changes in the underlying stock price) curves across all simulations show a decline as the option approaches maturity, reflecting that the option is moving closer to expiration and that the delta of an at-the-money option will tend towards 0.5. As the number of hedging steps increases, the delta becomes more finely adjusted. For higher N values, delta oscillates less, suggesting that more frequent re-hedging allows for better tracking of the option's exposure to the underlying asset. Additionally, the stock holding ϕ_t represents the amount of the underlying stock held to hedge the option position. As expected, ϕ_t decreases over time as the delta of the option falls. The holding starts higher at the beginning of the option's life and declines towards zero as the option reaches maturity. In simulations with more hedging steps ($N = 210, 420$), the stock holding is adjusted more frequently, leading to a smoother curve. This shows that frequent rebalancing helps maintain a better delta-neutral position. Furthermore, the bond holding $\psi_t B_t$ complements the stock holding to maintain the overall hedged portfolio. The bond holdings are negative, indicating that the strategy involves borrowing to finance the stock purchases. As with stock holdings, more frequent hedging results in smoother bond holding curves. In the simulations with more steps, the bond holding is updated more continuously, reflecting finer adjustments in the portfolio's bond exposure. In addition, the hedged portfolio value should ideally remain constant if the delta hedging strategy perfectly offsets the option's risk. In the simulations, the hedged portfolio value fluctuates but tends to stabilise as the number of hedging steps increases. For $N = 21$, the hedged portfolio exhibits larger swings, indicating greater deviations from perfect hedging due to infrequent rebalancing. As N increases, the portfolio value becomes more stable, suggesting that more frequent adjustments help maintain a closer hedge. Finally, the hedging error measures the difference between the theoretical hedge and the actual hedged portfolio. For simulations with fewer steps ($N = 21, 42$), the hedging error is more volatile, reflecting larger discrepancies due to less frequent adjustments to the portfolio. As N increases, the hedging error decreases, and its volatility diminishes. This demonstrates that more frequent rebalancing leads to better risk management, reducing the error between the actual portfolio value and the theoretical hedge.

Overall, these results highlight the importance of the frequency of rebalancing in a dynamic delta hedging strategy. With fewer steps (e.g., $N = 21$), the hedged portfolio and hedging error exhibit more significant fluctuations, indicating suboptimal risk management. As the number of hedging steps increases, the portfolio becomes more stable, and the hedging error decreases, showcasing the advantages of more frequent re-hedging in maintaining a delta-neutral portfolio and minimising risk exposure.